

## Enthalpic Relaxation and the Glass Transition in Polymer Blends

James N. Hay\* and Michael J Jenkins

The School Of Metallurgy and Materials, University of Birmingham,  
Birmingham B15 2TT, U.K.

**SUMMARY:** The kinetics of enthalpic relaxation are reviewed and applied to the ageing of a range of blends made from polyether imide and polyether ether ketone. DSC has been used to follow the development of enthalpic relaxation and a Williams-Watt stretched exponential equation relating the extent of relaxation,  $\phi(t)$ , to the ageing time  $t$  and an average relaxation time,  $\tau_a'$ , has been used to quantify the ageing process.

$$1 - \phi(t) = \exp\left(-\frac{t}{\tau_a'}\right)^{\beta'} \quad (1)$$

where  $\beta'$  is inversely related to the breadth of the relaxation spectrum such that  $0 < \beta' < 1.0$ . The relationship was modified to incorporate non-linearity in the relaxation behaviour.  $\phi(t)$  was measured directly from the enthalpy change observed in the endotherms on heating aged specimens through the glass transition in the DSC.

The PEI/PEEK blends were compatible over the full composition range in that they exhibited a single glass transition with a temperature that varied almost linearly with composition between those of the homopolymers. Enthalpic relaxation was found to be a useful technique for probing the molecular relaxations of polymer blends and confirming the degree of compatibility of the system. The  $\beta'$  values changed systematically with the blend composition between those of the homopolymers suggesting that the breadth of the relaxation spectra were similar in the blends to that in the homopolymers.

Physical ageing was observed to embrittle the blends, and there was a close correlation between the extent of enthalpic ageing and the change in mechanical and impact behaviour. The yield stress increased and the elongation to break decreased progressively with  $\phi(t)$  in addition to a reduction in impact strength.

The model of enthalpic relaxation and the kinetic relationships, outlined above, have been used to determine the onset of the glass transition temperature and subsequent progress of enthalpic relaxation at fixed ageing temperatures, for direct comparison with the change in specific heat observed in DSC experiments. Good agreement was observed between experiment and calculated glass transitions and the effect of variables, such as activation enthalpies, pre-exponential factors, non-linear factors such as  $X$  and  $\beta'$  and fictive temperature on the observed glass transition temperatures and the temperature range over which the glass transition occurred determined. Modifications to the model for the enthalpic relaxation have been suggested.

## Introduction

At temperatures below their glass transition temperature,  $T_g$ , amorphous solids are not in thermal equilibrium and physical properties which are greater than their equilibrium values decrease on storage towards the equilibrium values at rates which decrease with the temperature, and undercooling from the glass transition temperature. The change in material properties, such as yield stress, fracture toughness, creep compliance and Young's modulus with time is the phenomenon of physical ageing<sup>1</sup>. This change in material properties implies that physical ageing has considerable commercial importance in that material properties of thermoplastics are time dependent and for this reason has been widely studied.

When a liquid is cooled a temperature is eventually reached when the conformational relaxations of the molecules are too slow for the equilibrium conformations to be achieved within the time scale of cooling and so they do not continue to follow the temperature decrease. A glass transition occurs at this temperature and the conformations adopted by the molecules become fixed at this temperature. The conformations are thus cooling rate dependent and in a polymer the long ranged segmental motion of the chains are considered to cease at this temperature.

A useful concept in defining the onset of the formation of a glass<sup>2,3</sup> is that of free volume, in that the change in free volume decreases to zero at the glass transition temperature,  $T_g$ , and there is a marked change in the coefficient of cubic expansion above and below  $T_g$ . This description of the glass forming process is kinetic in nature, and the measured  $T_g$  and free volume are cooling rate dependent.

This description gives a ready explanation of physical ageing, as the progressive relaxation in material properties of a glass with storage as it slowly changes from those of the quenched glass towards the equilibrium liquid.

This paper considers the effect of composition on the development of physical in polymer blends to determine if it can be used to assess the extent of miscibility of the components and determine the change in material properties. To this end the compatible system polyether imide/ polyether ether ketone was examined in some detail.

## Experimental

A commercial grade of PEI, Ultem 1000, was used as supplied by GEC Ltd. The grade had a number average molecular weight of  $20 \text{ kg mol}^{-1}$ . It was dried prior at  $140^\circ\text{C}$  for 4 h. prior to processing.

PEEK, grade 450G, was supplied as a research sample by Victrex plc. This grade had a number average molecular weight of 40.7 and a weight average of  $99.2 \text{ kg mol}^{-1}$ . It was dried at  $160^\circ\text{C}$  for 4 hours prior to processing.

Blends were prepared by weight using an APV model MP2000 twin screw extruder with the zone temperatures of  $380^\circ\text{C}$  and at high torque. The dried blends and homopolymers were compression moulded into  $150 \times 150 \times 1 \text{ mm}$  plaques using a George Moores Ltd hydraulic press at  $380^\circ\text{C}$  for 2 minutes before quenching into ice water. The plaques were amorphous as measured by clarity, WAX ray scattering and DSC studies.

A Perkin-Elmer differential scanning calorimeter, model 2, was used interfaced to an IBM compatible PC. The DSC was used to measure the thermal characteristics of the polymer blends, as described elsewhere<sup>4</sup>. Disc samples, 10 -20 mg, were cut from the moulded plaques and encased in aluminium pans. An empty aluminium pan was used as a reference. The temperature scale of the DSC was calibrated from the melting points of standard metal specimens, indium, tin and lead. Power calibration was achieved using the enthalpy of fusion of 99.999% pure indium. This was taken to be  $28.45 \text{ J g}^{-1}$ .

Tensile tests were carried out on an Instron Testing machine, model TT-BM, capable of exerting a maximum load of 2500 Kg at cross-head speeds between 0.05 to  $500 \text{ mm.min}^{-1}$ . Dumbell test specimens BS 2782 type 301-A, were cut from the quenched plaques and aged in an oven as required.

Dynamic mechanical thermal analysis was carried out using a Polymer Laboratories, DMTA model 3, at flexing frequencies from 0.033 to 90 Hz. Measurements were carried out on 2 mm thick beams in flexure as a function of temperature. A heating rate of  $2^\circ\text{C.min}^{-1}$  was used for all these studies. Dielectric thermal analysis was carried out on a Polymer Laboratories DETA. It measured damping factor,  $\tan \delta$ , dielectric constant,  $\epsilon'$ , and loss permittivity,  $\epsilon''$ . Measurements were carried out over the frequency range 0.02 to 200 kHz at preset frequencies, from  $-150$  to  $300^\circ\text{C}$ .

## Results and Discussion

### a) The Kinetics of Physical Ageing

Hirai and Eyring<sup>5</sup> developed a model for the change in volume,  $V_h$ , of a glass at constant temperature,  $T$ , below the glass transition in terms of the free volume and fictive temperature,  $T_f$  and the internal pressure,  $p'$ , in order to quantify the relaxation of a glass with time at some temperature  $T$ , such that both  $T'$  and  $p'$  become  $T$  and  $p$  at equilibrium.  $p'-p$  becomes the excess pressure arising from the non-equilibrium distribution of free volume and so

$$p' = \frac{(V - V_f)}{(V_o \Delta\beta)} \quad (1)$$

where in terms of changes in the specific volumes,  $\Delta\beta$  is the difference in compressibility between the glass and liquid, and  $V_o$ ,  $V_f$  and  $V$  are the specific volumes initially, at equilibrium and at some intermediate time  $t$ . The change of fictive pressure at constant temperature,  $p'$ , occurs with a change in free volume, and

$$\frac{\delta p'}{\delta t} = \frac{2RT}{V_h \tau} \exp \frac{p' V_h}{RT} 2 \sinh \frac{p' V_h}{RT} \quad (2)$$

where  $\tau$  is the relaxation time of the single process.

There are two limiting solutions to equation 2 corresponding to,

$$p' V_h < RT \quad \text{i.e.} \quad -\frac{\delta p'}{\delta t} = \left(\frac{2}{\tau}\right) p' \quad (3)$$

and

$$p' V_h > RT \quad \text{i.e.} \quad p' = \exp\left(\frac{-2t}{\tau}\right) \quad (4)$$

Since  $(V_t - V_f)/(V_o - V_f) = \phi(t)$ , the extent the system is away from equilibrium, and inserting into equation 1 gives for equation (3)

$$\phi(t) = \exp\left(-\left(\frac{2t}{\tau}\right)\right) \quad (5)$$

and for equation (4)

$$\phi(t) = \left(\frac{RT\Delta\beta}{V_h}\right) \left(\frac{V_o}{\Delta V_o}\right) \ln\left(\frac{3t}{2\tau}\right) \quad (6)$$

where the change in volume is  $\Delta V_o = V_o - V_f$

Petrie and Marshall<sup>6</sup>, consider that physical ageing is best described as a retardation process such that the relaxation time decreases with conversion. Accordingly,

$$\phi(t) = \exp\left(-\left(\frac{t}{\tau}\right)\right) \quad (7)$$

and

$$-\frac{1}{\tau} = \frac{d}{dt}(\ln \phi(t)) = \frac{1}{t} \ln(\phi(t)) \quad (8)$$

Cowie and Ferguson<sup>10</sup> have modified the previous approaches by adopting a multi-relaxation model whereby physical ageing is not due to the relaxation of a single elementary process but to the relaxation of a distribution of processes, each characterised with their own relaxation time. Ageing is then the sum of all these relaxations with different time dependences, such that

$$\phi(t) = \sum_{\tau=-\infty}^{\tau=\infty} \rho(\tau) \exp\left(-\left(\frac{t}{\tau}\right)\right) d\tau \quad (9)$$

$\rho(\tau)$  is the distribution of states in the distribution and can be obtained through an inverse Laplace transform,  $\rho(\tau) = \left(\frac{1}{\tau^2}\right) L^{-1}[\phi(t)]$  where  $L^{-1}$  denotes an inverse Laplace transform.

Equation 5 has only been solved for a limiting case in a closed analytical form and  $\phi(t)$  is approximated by the stretched exponential form of the Williams-Watt<sup>11</sup> relaxation function, such that

$$\phi(t) = \exp\left(-\left(\frac{t}{\tau}\right)^\beta\right) \quad (10)$$

where  $\tau$  is an average relaxation time and  $\beta$  is an inverse measure of the breadth of the distribution of relaxation processes such that ( $0 < \beta < 1.0$ ), and for  $\beta = 1.0$  a single relaxation process is involved and as  $\beta \rightarrow 0$  the broader is the relaxation spectrum.

It has been pointed out by Hodge<sup>13</sup> that the average relaxation time,  $\tau$ , is time dependent and not constant, i.e.  $\tau = \tau_a t^\mu$ , where  $\mu$  is the relaxation time shift factor of Struik<sup>1</sup>.

This leads to a Williams -Watt function which accounts for non-linearity in the relaxation process,

$$\phi(t) = \exp\left(-\frac{t}{\tau'}\right)^{\beta'} \quad (11)$$

where  $\beta' = (1-\mu)\beta$  and  $\tau' = (1-\mu)\tau_a$

Despite the comments made by Hodge equation 11 is identical in time dependence to 10 since  $1-\mu$  is constant, i.e. close to 1.0 for most retardation process in polymers<sup>1</sup> and does not lead to a time dependent  $\tau'$ .

The concept of a non-linearity parameter,  $x$ , such that  $0 < x < 1.0$ , in physical ageing was introduced by Tool<sup>14</sup>, Narayanaswamy<sup>15</sup> and Moynihan et al.<sup>7</sup> for inorganic glasses in a modified form of the Arrhenius dependence of  $\tau'$  with ageing temperature,  $T$ , i.e.

$$\tau' = A \exp \frac{\Delta H}{R} \left( \frac{X}{T} + \frac{1-X}{T_f} \right) \quad (12)$$

where  $\Delta H$  is the activation enthalpy for the relaxation process,  $A$  is a pre-exponential factor and  $T_f$  is the fictive temperature as defined above. Equation 12 separates the temperature and structure dependences of the relaxation time.

The success or otherwise of these various rate expressions in describing the enthalpic relaxation of PEI and its blends with PEEK has been considered in some detail.

## b) The Kinetics of Enthalpic Relaxation.

The enthalpies of the glass,  $H_g(T)$ , and liquid,  $H_l(T)$ , have different temperature dependences, see Figure 1 and  $T_g$  is defined as the temperature at which  $H_g(T) = H_l(T)$ .

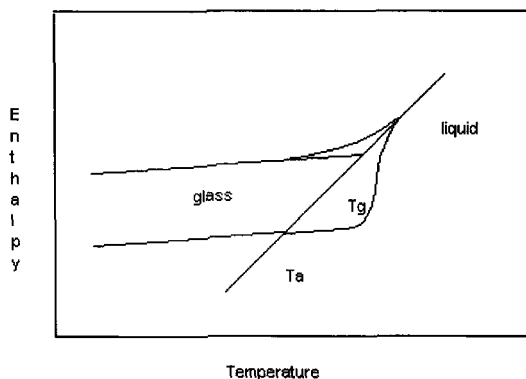


Figure 1. Temperature dependence of enthalpy

Since the heat capacities  $C_p$  for the liquid and glass are also temperature dependent, i.e.

$$C_p = dH/dT = a + bT + \text{etc.} \quad (13)$$

where  $a$  and  $b$  are constant, the difference in heat capacities,  $\Delta C_p$  is temperature dependent.

The step change in heat capacity between the liquid and the glass at  $T_g$ , i.e.  $\Delta C_p(T_g)$ , is then

$$\Delta C_p(T_g) = \Delta a + \Delta b T_g \quad (14)$$

where the  $\Delta$  terms arise from the difference in the value of the  $a$  and  $b$  parameters for the liquid and the glass at  $T_g$ . From Figure 1 it can be seen that the enthalpic relaxation at temperature,  $T_a$ , is accompanied with a progressive decrease in enthalpy of the glass from an initial value of  $H_g(T_a)$  to a final value at equilibrium of  $H_l(T_a)$ . The maximum change in enthalpy is,

$$\Delta H_{\max} = H_l(T_a) - H_g(T_a) = H_l(T_g) - H_g(T_g) + \Delta a(T_g - T_a) + \Delta b/2(T_g - T_a)(T_g + T_a)$$

Since,

$$H_l(T_g) = H_g(T_g) \text{ and } (T_g + T_a) \approx 2 T_a$$

then

$$\begin{aligned}\Delta H_{\max} &\approx \Delta a(\Delta T) + \Delta b(\Delta T) T_a \\ &\approx C_p \cdot \Delta T\end{aligned}\quad (15)$$

where

$$\Delta T = (T_g - T_a)$$

In terms of enthalpic relaxation, the extent of relaxation towards equilibrium, is

$$\phi(t) = \left(1 - \frac{\Delta H_t}{\Delta H_{\max}}\right) = \exp\left(-\frac{t}{\tau}\right)^\beta \quad (16)$$

where  $\Delta H_t$  is the enthalpy change on ageing for time  $t$ , at constant temperature,  $T_a$ .

### c) Physical Ageing Studies on the Blends.

The thermal response of the 50:50 PEI/PEEK blend, determined by DSC, is shown in Figure 2 as a plot of specific heat against temperature. It was typical of all the blends in showing several transitions. A glass transition was observed by a step change in heat capacity at 450 K, followed at about 50K higher temperature by an exotherm due to crystallisation of the PEEK component and at an even higher temperature by melting of the crystalline PEEK. Correcting for the heat capacity differences between the crystalline and amorphous PEEK the enthalpies of crystallisation and fusion were equal and so the original samples were amorphous. In all the blends only one glass transition was observed. The values were measured on the quenched blends using the procedures outlined by Aras and Richardson<sup>17</sup>, which was equivalent to equating the enthalpy of the liquid and the glass.

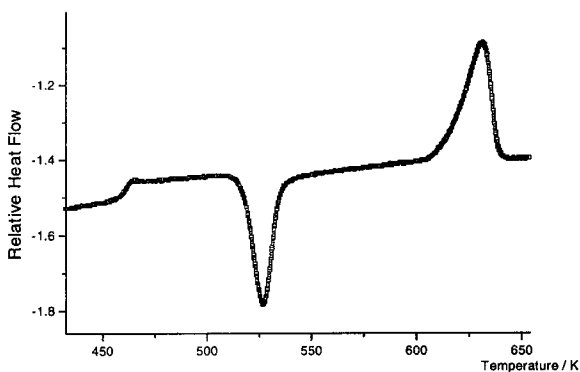


Figure 2. A DSC analysis of a 50:50 PEEK:PEI blend

The measured values of  $T_g$  for an individual blend varied with heating rate at constant sample



weight or with weight at constant rate due to thermal lags in the calorimeter and a correction was made for thermal lag by extrapolating to zero rate with constant sample weight. The corrected Tgs measured on the quenched samples varied with composition between the two homopolymers, PEEK at 418 and PEI at 489 K. The presence of a single glass transition observed at all blend compositions and varying progressively with composition is characteristic of a completely miscible blend system, see figure 3. These corrected values of Tg obtained on heating at constant composition also varied with rate of cooling prior to the measurement. Arrhenius plots of  $\log(\text{cooling rate})$  against the reciprocal of the Tg were linear with slopes equivalent to activation enthalpies for the glass forming process which varied with composition but between 800 - 1200 kJ.mol<sup>-1</sup>.

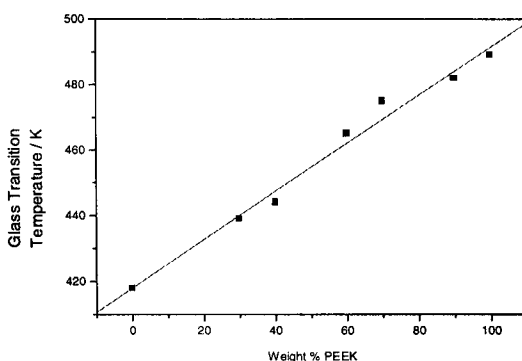


Figure 3. Variation of Tg with composition of the blends

The temperature dependence of the heat capacities of the various blends were also measured on quenched and aged glasses from well below Tg and on the liquid above Tg but below the crystallisation temperature. This limited the temperature range above Tg due to the onset of crystallisation of the PEEK component. Corrections were again made for thermal lags as described above. The heat capacities were unaffected by ageing, see Table 1a. Linear dependences of heat capacity were observed for the glass and liquid phases and a least square fit used to determine the coefficients, a and b, at each composition, see Table 1b, for,  $C_p = a + bT$ .

From these values of the coefficients  $\Delta C_p(T_g)$  was determined for each composition. These values varied with composition reaching a maximum at 50:50 blend of 0.297 J.g<sup>-1</sup> and varying between the limits of 0.210 J.g<sup>-1</sup> for PEI and 275 J.g<sup>-1</sup> for PEEK, see Figure 4.

Table 1. Heat Capacities of the blends

a) The effect of ageing on PEI

Ageing Time	1400 min		30000 min	
Temperature / K	Cp quench / J.g <sup>-1</sup> ± 5%	Cp aged / J.g <sup>-1</sup> ± 5%	Cp quench / J.g <sup>-1</sup> ± 5%	Cp age / J.g <sup>-1</sup> ± 5%
490	1.67	1.68	1.66	1.69
485	1.64	1.65	1.64	1.65
480	1.62	1.63	1.63	1.63
475	1.61	1.61	1.61	1.61
470	1.58	1.59	1.59	1.58
465	1.55	1.56	1.57	1.56

b) Temperature dependence of the heat capacities

Composition	Glass	Glass	Liquid	Liquid	
Wt % PEI	a	b	A	B	ΔCp(Tg) ± 5%
60	-140	3.925	280	3.66	295
70	-200	4.07	210	3.76	270
80	-150	3.03	160	2.52	230
100	-130	3.89	420	3.19	210

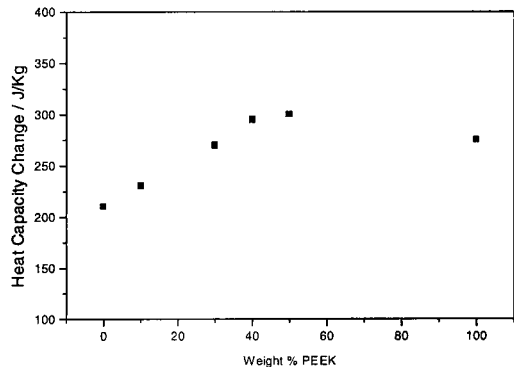


Figure 4. Composition dependence of the change in heat capacity at Tg

Quenched samples of the blends were stored in the DSC at various ageing temperatures,  $T_a$ , and for various storage times. On quenching the samples at  $180\text{ K.min}^{-1}$  to 300 K and subsequent heating an endothermic process was observed at the glass transition, which developed in size and moved to higher temperatures with increasing ageing time,  $t_a$ . This can be seen for a 50:50 blend in Figure 5 and is characteristic of all the blends studied. The area under the endotherm is the enthalpy recovered on reheating the aged material through the glass transition as shown in Figure 1 and is a measure of the enthalpy change,  $\Delta H_t$ , due to the amount of relaxation which had occurred on storage.

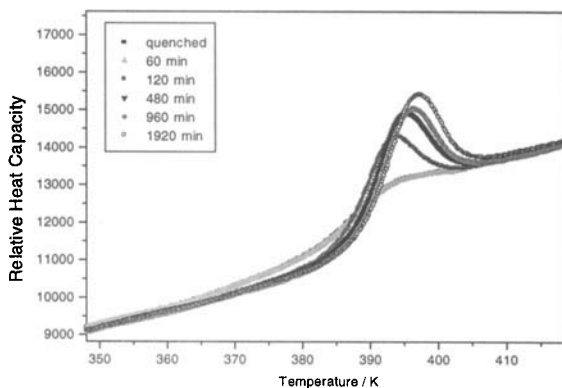


Figure 5. The development of the ageing endotherm with storage time

$\Delta H_t$  was determined by subtracting the area between the specific heat-temperature curves of the quenched and aged specimens, between two fixed temperatures on either side of the transition. The exponential increase in  $\Delta H_t$  with time can be seen in Figure 6 as well as the effect of changing  $T_a$ .

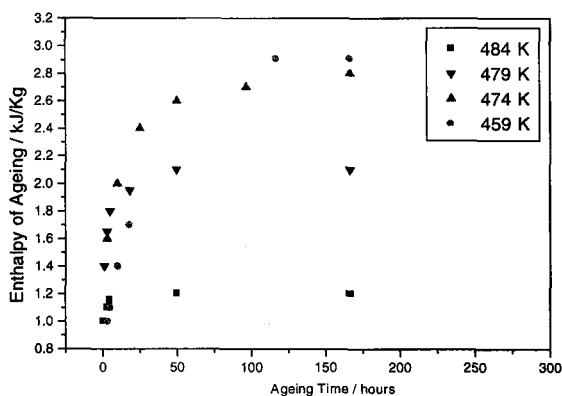


Figure 6. The change in ageing enthalpy with time

The rate of development of  $\Delta H_t$  with time decreased with  $T_a$ , and reached a limiting value of  $\Delta H_{\max}$  at long ageing periods. Using the limiting experimental values of  $\Delta H_t$  as a measure of  $\Delta H_{\max}$ , the validity of equation 10 was determined from a plot of  $\Delta H_{\max}$  against  $\Delta T$ . A linear relationship was observed up to  $\Delta T$  values of 15-20 K, see figure 7, and marked deviations from the linear dependence was observed beyond this.

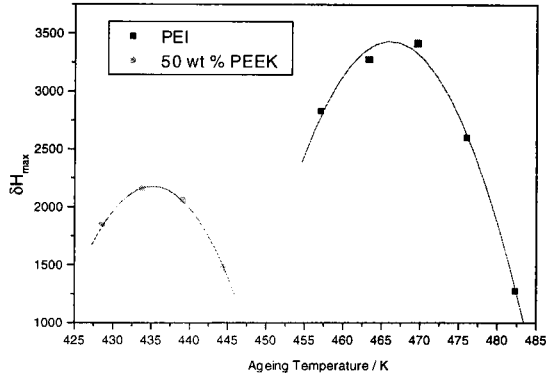


Figure 7. The temperature dependence of the maximum enthalpy

The drop in value may reflect the greater storage times required to reach equilibrium and the  $\Delta H_{max}$  observed were underestimated. The initial slope of the observed linear dependence was comparable in value to that of  $\Delta C_p$  as listed in Table 2, and so  $\Delta C_p \cdot \Delta T$  was a good estimate of  $\Delta H_{max}$ .

Table 2. Comparison of  $\Delta H_{max}$  and  $\Delta C_p \cdot \Delta T$

Blend Composition	$\Delta T / K$	$\Delta H_{max} / J \cdot g^{-1}$	$\Delta C_p \cdot \Delta T / J \cdot g^{-1}$
100	5	1.20	1.10
	10	2.10	2.20
	15	2.80	3.10
	20	3.00	4.20
	30	3.00	6.30
90	5	1.15	1.15
	10	2.20	2.30
	20	3.40	4.60
70	5	1.50	1.35
	20	3.90	5.40
	30	3.50	8.10

Using the Marshall and Petrie model,  $\tau$  was calculated as a function of the extent of relaxation,  $\phi(t)$  and the values were observed to vary by several orders of magnitude over the course of the process, see Figure 8.

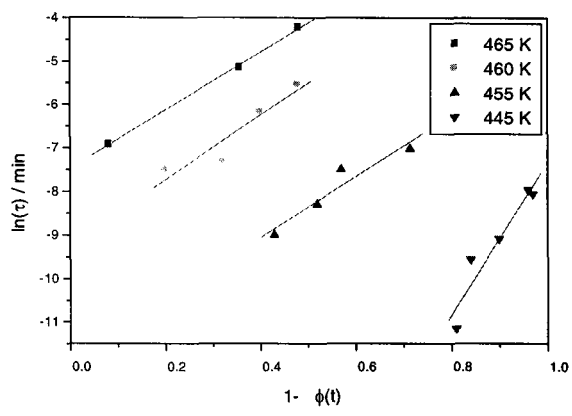


Figure 8. The change in relaxation time with conversion for a 30% PEI blend.

From the Arrhenius relationship,

$$-\ln(\tau) = \ln(A') + C(\Delta H_{\max} - \Delta H_t)$$

where  $\ln(A') = \ln(A) + \Delta H_a/RT$

the C paramater and the activation enthalpies,  $\Delta H_a$ , were determined, see Table 3 .

Table 3. Analysis of Enthalpic Relaxation Data

Blend Composition wt % PEI	Ageing Temperature / K	C / g J <sup>-1</sup>	Ln A'	Ln A	Eh / kJ.mol <sup>-1</sup>
100	484	7	-4.91		
	479	2.7	-5.88		
	474	2.3	-8.77	245	1000
	469	2.5	-12.54		
	459	1.8	-16.6		
90	473	5.4	-5.8		
	468	1.4	-7.96	258	1050
	462	1.3	-11.37		
70	465	6.7	-7.26		
	460	3.5	-10.35		
	455	2	-11.4	235	1000
	150	1.1	-15.4		
	445	0.9	-15.2		
50		2.89		520	1900
0		2.29		314	1080

The values of C increased with increasing PEEK concentration and the activation enthalpies were similar to those determined from the cooling rate dependence of the glass transition, see Table 4. The characteristic feature of the Petrie and Marshall model is the large change in relaxation time, covering several decades, with the development of enthalpic relaxation.

Table 4. Dependence of Tg of PEI on Cooling Rate

Cooling Rate / K.min <sup>-1</sup>	Tg / K ± 0.5
160	486.3
80	485.8
40	483.8
20	480.7
10	479.7
5	478.7
2.5	478.2
1.25	475.1
0.62	472.8
0.31	472.6

The Cowie and Ferguson equation was also used to analyse the same experimental data, of  $\phi(t)$  against  $t$ . Linear plots of  $\log -[\ln \phi(t)]$  against  $\ln(t)$  were obtained consistent with equation 11, with slopes which corresponded to the value of  $\beta'$  and intercept at  $t=1$  of  $\tau'$ . In this analysis  $\Delta H_{\max}$  was taken to be the observed experimental limit of  $\Delta H_t$ . Reduced variable plots  $\log -[\ln \phi(t)]$  against  $\ln(t/\tau')$  are shown for the blends in Figure 9.

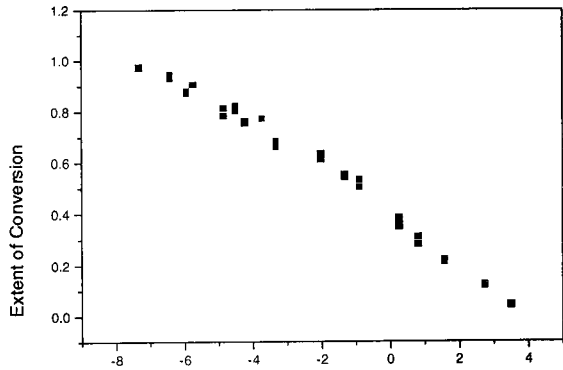


Figure 9. Reduced variable plot. Extent of enthalpic relaxation against reduced time

The superposition of the data was consistent with a constant  $\beta'$  value over the range of temperatures studied. The values of  $\beta'$ ,  $\tau'$  and  $\Delta H_{\max}$  were also determined by curve fitting the data, using them as adjustable parameters in a non-linear curve fitting procedure, the fitted values are listed in Table 5. The activation enthalpies were determined from the temperature dependence of  $\tau'$ . These values were consistent with those determined by the Marshall and Petrie analysis and also from the cooling rate dependence of the glass transition.

Table 5. Williams-Watt Fit of the Enthalpic Relaxation Data

a) Using  $\Delta H_{\max} = \Delta C_p \Delta T$

Blend Composition wt % PEI	Ageing Temperature	$\beta'$	$\tau'$	$\Delta H_a$	Average $\beta'$
0	484	0.34	10.0		
	479	0.31	40.0		
	474	0.31	470		
	469	0.29	6800		
	459	0.25	200000	$800 \pm 200$	0.28
90	473	0.59	340		
	468	0.43	850		
	462	0.34	2000	$700 \pm 200$	0.45
70	465	0.29	15		
	455	0.27	4300		
	450	0.32	75000		
	445	0.32	226000	$1000 \pm 200$	0.29

b) Using  $\Delta H_{\max} = \text{Experimentally Observed Value}$

Blend Composition wt % PEI	Ageing Temperature	$\beta'$	$\tau'$	$\Delta H_a$	Average $\beta'$
0	484	0.39	20.0		
	479	0.43	30.0		
	474	0.41	170		
	469	0.42	520		
	459	0.44	1800	$370 \pm 100$	0.40
90	473	0.65	180		
	468	0.45	500		
	462	0.47	1600	$360 \pm 100$	0.55
70	465	0.37	30		
	455	0.35	170		
	450	0.21	1400		
	445	0.41	2400	$430 \pm 100$	0.55

The  $\beta'$  values and activation enthalpies varied progressively with blend composition and were consistent with a compatible homogeneous system, in that similar studies on crystalline blend samples produced lower  $\beta'$  values, as low as 0.2 suggesting that heterogeneous systems produced very low values and those of the amorphous blends were consistent with a homogeneous system.

### **Simulation of the Glass Transition.**

The dependence of the  $T_g$  on cooling rate has the same activation enthalpy as that of enthalpic relaxation and it has been suggested<sup>18</sup> that enthalpic relaxation is an extension of glass formation. Accordingly the kinetic relationships for enthalpic relaxation have been used to model the formation of the glass on cooling.

The liquid was considered to cool at a cooling rate,  $R$ , from a temperature  $T$  and the fictive temperature,  $T_f$ , was used to monitor the transition since if  $T=T_f$  then the system is a liquid. If  $T < T_f$  the liquid is converting to the glass and if  $T_f$  does not change with further cooling the glass has formed.

A finite element calculation was used to follow the change in fictive temperature on cooling. The cooling rate,  $R$ , defined the dwell time,  $dt$ , at each temperature,  $T$ , and the extent of relaxation,  $d\phi$ , which develops at each temperature is defined by the Williams -Watts function,

$$\phi(t) = \exp\left(-\frac{t}{\tau'}\right)^{\beta'}$$

The relaxation time at each temperature is given by the modified Arrhenius relationship,



$$\tau' = A \exp \left[ \frac{X\Delta H}{RT} + \frac{(1-X)\Delta H}{RT_f} \right]$$

The change in fictive temperature,  $dT_f$ , accompanying a change in temperature,  $dT$ , was then calculated for each temperature,  $T$ , from,

$$dT_f = dT(1 - \phi(T, dt))$$

The relative change in heat capacity was defined as  $C'_p = dT_f/dT$  such that for the liquid  $C'_p = 1.0$  and for the glass  $C'_p = 0.0$ . During conversion  $C'_p$  from liquid to glass  $C_p$  varies from 1.00 to 0.0. The calculated fictive temperatures showed the classical variation with temperature expected, see Figure 10a, with two distinct temperature dependences corresponding to liquid and glass regions.

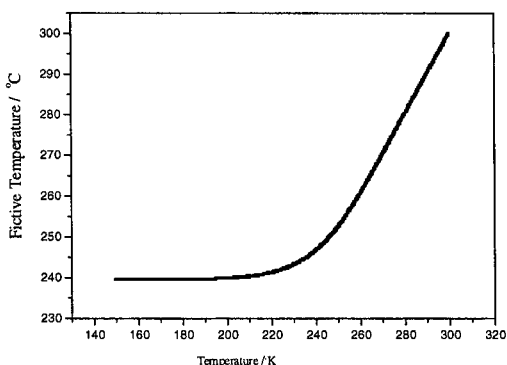


Figure 10a. Variation of fictive temperature on cooling

Extrapolation of the two linear regions defined the  $T_g$  from their intercept. The fictive temperature heat capacities also exhibited the characteristic step function at  $T_g$ , see Figure 10b.

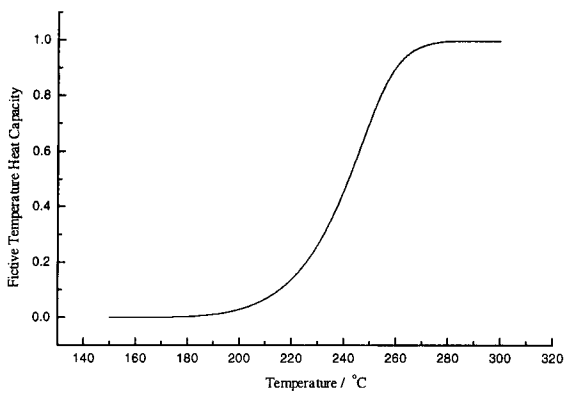


Figure 10b. Variation of fictive temperature heat capacity on cooling

It was observed that the value of  $T_g$  varied with cooling rate as determined by the value of the activation enthalpy selected, but the individual values changed according to the values selected for  $\ln A$ ,  $\Delta H_a$  and the  $X$  parameter, see Table 5.

Table 5. The Effect of Selected Variables on the Calculated Value of  $T_g$ .

a) Effect of varying the activation enthalpy,  $\Delta H_a$ .  $\ln A = -117$ ,  $X = 0.37$  and  $\beta = 0.38$

$E_a / \text{kJ} \cdot \text{mol}^{-1}$	$T_g^* / \text{K}$	$T_g^* / \text{K}$
300	277.78	279.72
250	232.06	234.27
200	185.32	187.27
150	140.60	140.68

b) Effect of varying  $X$ .  $\ln A = -117$ ,  $\Delta H_a = 258 \text{ kJ} \cdot \text{mol}^{-1}$  and  $\beta = 0.38$

$X$	$T_g^* / \text{K}$	$T_g^{**} / \text{K}$
1	246.91	246.42
0.8	245.29	244.76
0.6	243.02	242.82
0.4	240.11	241.71
0.2	236.01	238.39

c) Effect of varying  $\ln A$ .  $\Delta H_a=258 \text{ kJ.mol}^{-1}$ ,  $X=0.37$  and  $\beta=0.38$

$\ln A$	$T_g^* / \text{K}$	$T_g^{**} / \text{K}$
-200	147.31	148.17
-150	191.71	163.31
-100	274.14	191.84

d) Effect of varying  $\beta$ .  $\ln A=-117$ ,  $\Delta H_a=258 \text{ kJ.mol}^{-1}$  and  $X=0.38$

$\beta$	$T_g^* / \text{K}$	$T_g^{**} / \text{K}$
1	259.02	215.73
0.8	256.34	242.03
0.6	250.73	250.69
0.4	240.97	256.26
0.2	218.04	258.74

$T_g^*$  measured from intersection of fictive temperatures of liquid and glass

$T_g^{**}$  measured by Aras and Richardson's method

The effect of non-linearity in the enthalpic relaxation process on the shape of the glass transition and the temperature range over which it occurred was considered by altering the value of  $\beta'$  and  $X$  in turn. Lowering  $\beta'$ , corresponding to a broader distribution of relaxation times, lowered  $T_g$  as defined by the temperature corresponding to 50% conversion, and also produced a wider temperature range over which the transition was observed, see Figure 11, from over 100 K for  $\beta'$  values about 0.2 and 30 K for value of 1.0.

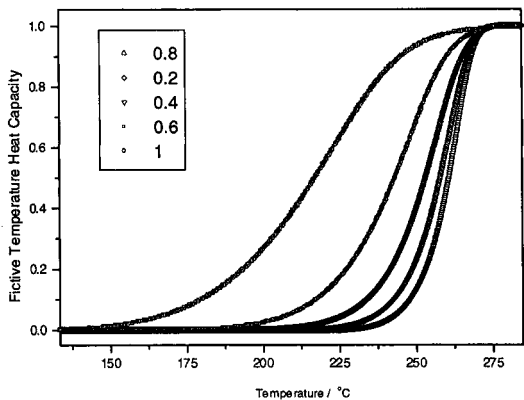


Figure 11a. Variation of the fictive temperature heat capacity with temperature. Effect of  $\beta$

The structure parameter  $X$  had a similar effect. It was not possible to separate either effects and the breadth of the glass transition was primarily determined by both  $X$  and  $\beta'$ .

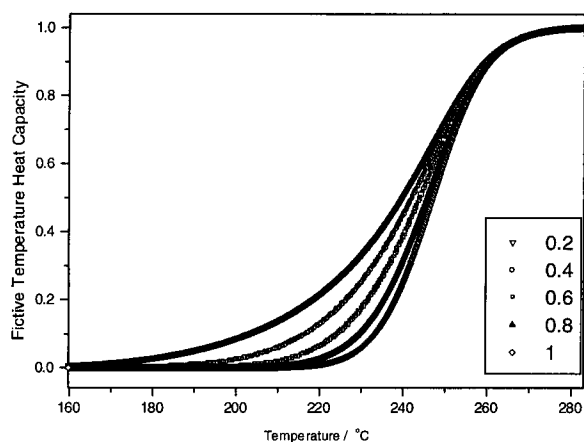


Figure 11b. Variation of fictive temperature heat capacity with temperature. Effect of  $X$

The progress of enthalpic relaxation was also calculated at constant  $T_a$  from the change in fictive temperature, using a constant relaxation time,  $\tau$ . Endotherms developed at the glass transition as observed experimentally on ageing a glass, see Figure 12a. In the finite element calculations, time intervals,  $dt$ , corresponding to linear steps in  $\phi(t)$  were chosen and the glass was allowed to reach within 1 % of equilibrium. Correction was made to the  $\tau$  values to allow for the change in fictive temperature during conversion and the effect of the  $X$  parameter on the change in relaxation time,  $\tau'$ .

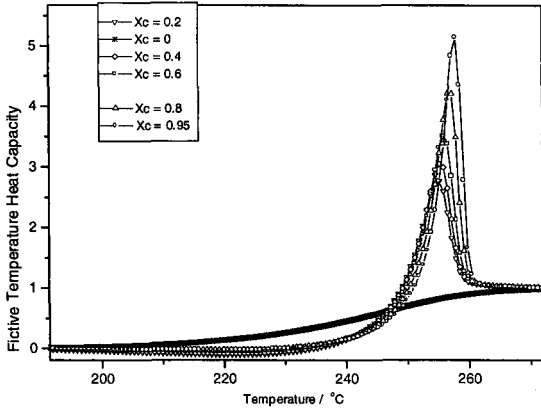


Figure 12a. Variation of the endothermic ageing peak on Tg with extent of conversion

$\beta'$ , and  $\tau'$  were calculated for each assumed value of  $X$ ,  $\beta$ ,  $\Delta H_a$ , and  $A$  adopted in the calculation, see Table 6.

Table 6. The Effect of Non-linearity on the calculated average  $\beta$  value

a) A comparison of  $\beta$  values calculated and used in the calculation

$\Delta T = 5 \text{ K}$	$\beta$ used	0.10	0.20	0.30	0.40	0.50	0.60	0.70	0.80	0.90
	$\beta$ calc	0.096	0.18	0.27	0.35	0.42	0.49	0.55	0.61	0.67
$\Delta T = 10 \text{ K}$	$\beta$ used	0.10	0.20	0.30	0.40	0.50	0.60	0.70	0.80	0.90
	$\beta$ calc	0.092	0.17	0.24	0.24	0.3	0.36	0.41	0.45	0.53
$\Delta T = 20 \text{ K}$	$\beta$ used	0.10	0.20	0.30	0.40	0.50	0.60	0.70	0.80	0.90
	$\beta$ calc	0.09	0.15	0.20	0.24	0.28	0.31	0.33	0.35	0.37
$\Delta T = 50 \text{ K}$	$\beta$ used	0.10	0.20	0.30	0.40	0.50	0.60	0.70	0.80	0.90
	$\beta$ calc	0.07	0.11	0.13	0.14	0.16	0.16	0.17	0.18	0.18

b) Effect of non-linearity on observed  $\beta$  values.

$\Delta T / \text{K}$	$\beta$ used	$\beta$ calc
2	0.37	0.35
10	0.37	0.29
20	0.37	0.23
50	0.37	0.14

At small degrees of supercooling good agreement was observed between adopted and calculated values of  $\beta'$  but for values of  $\Delta T=20$  and greater the  $\beta'$  obtained by curve fitting deviated markedly from the value used in the calculations. This was also shown by the marked curvature in the  $\log(\ln(1-\phi(t)))$  plot against  $\log t$  which should be linear with a slope of  $\beta'$  for a constant relaxation time. Non-linearity produced by the X parameter was apparent at supercoolings above 20 K, see Figure 12b.

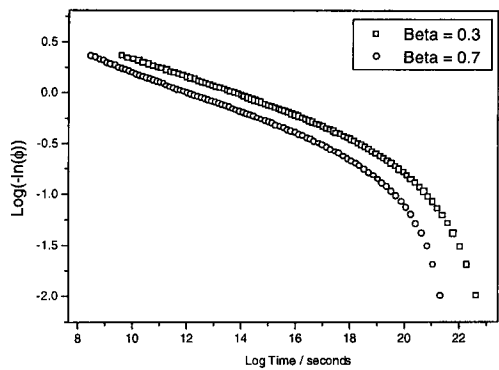


Figure 12b. A double logarithm plot for a supercooling of 50 degrees

A single  $\beta'$  value cannot be ascribed to the overall process as it changes with conversion. non-linearity arising from the X parameter made itself apparent in the change in  $\tau'$  as equilibrium is approached.  $\tau'$ , however, does not change as much as it does in the Marshall and Petrie model, from which it was apparent that  $\ln(t)$  changed linearly with conversion over the complete process. The overall effect of a non-constant  $\beta'$  value is to produce curvature in the reduced variable plot and to reduce  $\beta$ .

**Mechanical Properties and Ageing.**

Tensile tests were carried out on the quenched specimens. All the blend samples were ductile exhibiting well defined yield and drawing stresses and distinct neck profiles which propagated

through the specimens until fracture by growth of an edge diamond. The yield stress dropped progressively from  $95 \pm 5$  to  $60 \pm 5$  M Pa with PEEK content, see Figure 13.

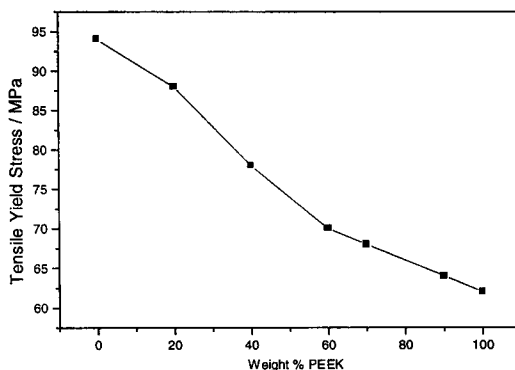


Figure 13. Variation of the yield stress with composition

On ageing the yield stress increased progressively and at the same time the elongation to break decreased. The neck profile as shown by the increased rate in drop of the engineering stress with strain increased as the neck became more localised. Samples with high yield stresses fractured in a brittle mode. Crazes were observed prior to yield and brittle fracture was initiated from these to develop. SEM analysis of the fracture surfaces confirmed the presence of the craze initiated fracture mechanism. In all the blends the yield stress increased with storage time at various temperatures and developed with the increase in enthalpy of ageing and the ageing time, see Figure 14.

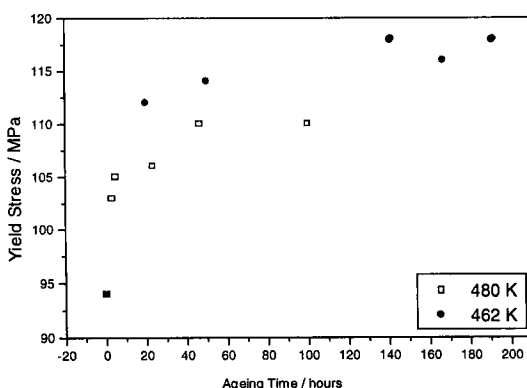


Figure 14. The change in yield stress with ageing time

Tensile yielding appeared to destroy physical ageing in that samples taken from the necked regions of the yielded material exhibited no ageing endotherms at  $T_g$  and appeared to be identical to the quenched sample to the DSC analysis. Similar effects were observed in the impact behaviour of the blends. PEI and the blends were observed to be notch sensitive and in a Charpy impact test at 0.25mm notch tip radius they fractured in a brittle mode with low impact strength,  $3.5 \text{ J.m}^{-2}$ . Mixed mode fracture was observed at higher notch tip radius as yielding increasingly contributed to the impact strength. Ageing the specimens prior to notching and impact reduced the impact strength at the higher notch tip radii consistent with the increased yield stress and the general embrittlement of the materials on ageing.

DMTA analysis of the blends showed that the flexural modulus, at 1 Hz and 298 K, changed progressively with composition from  $3.4 \pm 0.3$  to  $2.6 \pm 0.2 \text{ G Pa}$  for the quenched blends. No difference in the moduli was observed on ageing within the experimental scatter. The temperature corresponding to a maximum value in  $\tan \delta$  was considered to be a measure of  $T_g$  at the imposed frequency. These temperatures at constant frequency varied with compositions, consistent with the DSC observations discussed above. The compositional dependence of the observed  $T_g$ s were fitted to a Gordon-Taylor relationship incorporating two interaction parameters,  $K_1$  and  $K_2$ , i.e.

$$(T_g - T_{g1})/(T_{g2} - T_{g1}) = (1 + K_1) W_1 - (K_1 + K_2) W_1^2 + K_2 W_1^3$$

where  $W = (K W_2 / (W_1 + K W_2))$ , and  $K = K' T_{g1}/T_{g2}$  and  $K' = p_1 / p_2$ .

$W_1$  and  $W_2$  are the weight fraction of the components 1 and 2 with densities  $p_1$  and  $p_2$  and  $T_{g1}$ ,  $T_{g1}$  and  $T_{g2}$ . Negative deviation was observed with  $K_1 = 0.320 \pm 0.005$  and  $K_2 = 0.111 \pm 0.002$ . The observed  $T_g$ s varied with frequency from which the activation enthalpies of the glass transitions were determined over the frequency range, 0.033 to 90 Hz, from the Arrhenius relationships. A similar study has been carried out<sup>19</sup> by DETA and the measurement



of  $T_g$  defined by the maximum in  $\tan \delta$  extended over the frequency range 0.03 to 300 kHz. The activation enthalpies measured for each blend were very similar to those determined by DMTA, between 800 to 1250 kJ mol<sup>-1</sup>.

## Discussion.

The activation enthalpies for glass formation and relaxation are very similar and independent of the method chosen to measure them. Accordingly a master Arrhenius plot incorporating all this data, i.e. the variation of  $T_g$  measured by DMTA and DETA at different frequencies, the dependence of  $T_g$  on cooling rate as measured by DSC, and the observed dependence of the enthalpic relaxation times on ageing temperature, was constructed by using a vertical shift factor on the  $\log(\tau)$  axis. This is consistent with a Williams-Landel-Ferry equation<sup>20</sup> for relaxation times,  $t$  at temperature  $T$  and to at  $T_0$ , such that

$$\ln(\tau/\tau_0) = -C(T-T_0)/(C_2+T-T_0)$$

and superposing the observed linear dependences on one another at a reference temperature,  $T_0$ . This master curve, see Figure 15, defines the relaxation time of the glass at each temperature and over 10 decades of relaxation times are covered. The curve defines the measured value of  $T_g$  corresponding to the time scale of the experimental technique used in its measurement and implies that enthalpic relaxation is an extension of the glass formation process.

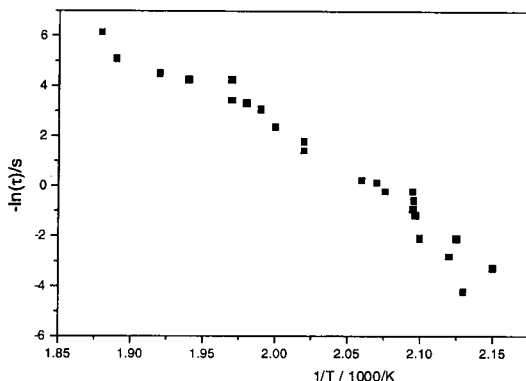


Figure 15. Master curve relaxation time and temperature plot for PEI

Of the various kinetic relationships derived it is apparent that the Cowie-Ferguson approach in which a wide range of molecular processes are allowed to relax is the most powerful in modelling the glass formation process. The stretched exponential function does appear to account for the time dependence of the degree of conversion at various temperatures. The assumption of a constant average relaxation time for the ageing process appears to be invalid.

However, incorporating the approach adopted by Hodge and O'Reilly does not change this assumption but merely redefines a different average for the average relaxation time,  $\tau'$ , and also for  $\beta'$ . Using the retardation model as outlined by Petrie and Marshall, in turn, does not appear to be helpful since it produces too wide a variation in the relaxation time with conversion. For the model it is observed to change by several order of magnitudes. The effect of non-linearity on the progress of the enthalpic relaxation as introduced by the structure factor,  $X$ , has been computed. Essentially as the glass relaxes, the fictive temperature,  $T_f$ , changes from a value close to  $T_g$  to the ageing temperature,  $T_a$ , and as defined by equation 12 the average relaxation time changes. This depends on the degree of supercooling, i.e. the difference between  $T_g$  and  $T_a$ . At low values of  $\Delta T$  the assumption of constant  $\tau_a$  is approximately correct and the modified stretched exponential function fits the data well and

the  $\beta$  and  $\tau$  determined from the analysis have some significance. This is not the case at high values of  $\Delta T$  where marked deviations are observed with reduced values determined for  $\beta'$  and  $\tau$ . Most deviations occur in analysing the enthalpic relaxation data at high  $\Delta T$ s. This has invariably been attributed to deviations in  $\Delta H_{\max}$  from  $\Delta C_p \cdot \Delta T$  and to the difficulty in determining  $\Delta H_{\max}$  at long storage times. The kinetic relationships have been used to compute the glass transition on cooling a liquid. The temperature range over which the transition is observed experimentally is closely related to the breadth of the relaxation spectrum,  $\beta$ , and to structure parameter  $X$ . It is apparent that these parameters could be determined directly from the breadth of the transition as determined by DSC.

## References.

1. L.C.E. Struik, "*Physical Ageing of Amorphous Polymers and other Materials*", Elsevier, New York and Amsterdam, (1978).
2. A. J. Kovacs, *Forsch. Hochpolym.-Forsch*, **3**, 394, (1963).
3. R.N. Haward, "*The Physics of Glassy Polymers*", Applied Science Publishers Ltd., London, (1973).
4. J.N. Hay, *Pure and Appl. Chem.*, **67**, 1855, (1995).
5. N. Hirai and H. Byring, *J. Appl. Physics*, **29**, 810, (1958); *J. Appl. Physics*, **37**, 51, (1959).
6. A.S.Marshall and S.E.B. Petrie, *J.Appl. Physics*, **46**, 4223, (1975).
7. C.T. Moynahan, A.J.Easteal, M.A. DeBolt and J Tucker, *J. Amer. Ceram. Soc.*, **59**, 12, (1976).
8. I.M. Hodge, *Macromolecules*, **16**, 898, 91983).
9. A.J. Kovacs, J.J. Aklonis, J.M. Hutchinson, and A.R. Ramos, *J. Polym. Sci., Poly. Phys. ed.*, **22**, 1097, (1984).
10. J.M.G. Cowie and R. Ferguson, *Polym. Comm.*, **27**, 258, (1986).

11. F. Kohlrausch, *Annalen der Physik und Chemie*, **128**, 1, (1866).
12. G. Williams and D.C. Watts, *Trans. Faraday Soc.*, **66**, 80, (197)
13. I.M. Hodge and J.M. O'Reilly, *Polymer Letters*, **33**, 4883, (1992)
14. A.Q Tool, *J.Amer. Ceram. Soc.*, **29**, 240, (1946).
15. O.S. Narayanaswamy, *J. Amer. Ceram. Soc.*, **54**, 491, (1971).
16. A.A. Mehmet-Alkan and J.N. Hay, *Polymer*, **33**, 3527, (1992)
17. L. Aras and M. J. Richardson, *Polymer*, **31**, 1328, (1990)
18. A. A. Goodwin and J. N. Hay, *Polymer Comm.*, **31**, 338, (1990).
19. F. Biddlestone, A.A. Goodwin, J. N. Hay, and G.A.C. Mouledous, *Polymer*, **32**, 3119, 1991
20. M. L. Williams, R. F. Landel and J. D. Ferry, *J. Amer. Chem Soc*, **77**, 3701, 1955